*Desalination and Water Treatment*
www.deswater.com

doi: 10.5004/dwt.2019.24710

172 (2019) 190–198
December

# Lactic acid recovery from water by Amberlite IRA-400

Nevriye Halilibrahimoğlu, İsmail İnci*, Nilay Baylan

*Department of Chemical Engineering, İstanbul University-Cerrahpaşa, Avcılar 34320, İstanbul, Turkey, Tel. +90 212 473 70 70/17674; Fax: +90 212 473 71 80; emails: isminci@istanbul.edu.tr (İ. İnci), nevriye92@gmail.com (N. Halilibrahimoğlu), nilay.baylan@istanbul.edu.tr (N. Baylan)*

Received 18 March 2019; Accepted 23 July 2019

**ABSTRACT**

The aim of this investigation is to recover lactic acid, which widely produced in aqueous solutions by fermentation processes, from water by Amberlite IRA-400. This separation is very important for the production of lactic acid because of the accumulation of lactic acid must be prevented for the fermentation process to be continued continuously. Amberlite IRA-400 is an ion-exchange resin used as an adsorbent in this separation study. Adsorption time, initial concentration of lactic acid, amount of Amberlite IRA-400 and temperature have been selected as the parameters affecting the adsorption process. The adsorption capacities of Amberlite IRA-400 under various conditions were detected and compared with each other. It has been determined that a significant lactic acid amount was recovered by Amberlite IRA-400. Langmuir, Freundlich and Temkin isotherm models were utilized to explain the adsorption mechanism. Kinetic models such as pseudo-first-order, pseudo-second-order kinetic models were used, and also, Weber-Morris intra-particle diffusion model was performed. Among the isotherms used, Freundlich isotherm model was found to fit the experimental results. Besides, the most favorable kinetic model was determined as pseudo-second-order kinetic model.

*Keywords:* Lactic acid; Amberlite IRA-400; Adsorption; Recovery

## 1. Introduction

Lactic acid is also known as alpha-hydroxy acid. It contains carboxylic and hydroxyl groups. These groups play significant roles in various chemical production processes. Lactic acid has been utilized as a raw material for polylactic acid production which is a biodegradable polymer. Furthermore, lactic acid is also used in the manufacture of many chemicals like pyruvic acid, acrylic acid, propionic acid, propylene glycol, acetaldehyde and, 2,3-pentanedione. It has also been utilized in various industries including food, pharmaceutical, cosmetic and textile industries [1].

Lactic acid can be acquired by either biological or chemical synthesis. However, it has been broadly produced in aqueous solutions by fermentation processes [2]. During the production of lactic acid by fermentation, pH change is very significant. Because, lactic acid accumulation during fermentation decreases pH of the fermentation broth and microorganism activity is reduced. Therefore, the accumulation of lactic acid must be prevented for the fermentation process to be continued continuously [3]. Also, lactic can be present in waste streams or effluents in numerous chemical industries. Because of these reasons, it is very significant to recover lactic acid from the water. To this end, different techniques are frequently utilized to recover lactic acid from the water like solvent extraction [4,5], reactive extraction [6,7], direct distillation [8], reactive distillation [9], reverse osmosis [10,11], electrodialysis [12,13], ultrafiltration [13,14] and adsorption [15,16]. Among these recovery techniques, adsorption has many benefits like a higher efficiency, easy handling, low capital, operating costs, quick response [17,18],

* Corresponding author.

*Presented at the 4th International Conference on Recycling and Reuse 2018 (R&R2018), 24–26 October 2018, Istanbul, Turkey*

1944-3994/1944-3986 

absence of sludge and harmful by-product generation [19]. This technique also can be integrated easily with the fermentation process [2]. The adsorption of lactic acid was examined by using various adsorbents like multiwall carbon nanotube [1], zeolite [20], activated carbon [2,21] and layered double hydroxide [16].

Amberlite IRA-400, a macroporous and strong base anion-exchange resin, can be used for the removal of certain ions from a solution by replacing them with other ions [22,23]. In other words, Amberlite IRA-400 can take place the adsorption by means of an ion exchange mechanism. So, it has been preferred in the adsorption process under different operating conditions. Besides, anion-exchange resins are non-toxic for microorganisms; hence they can be utilized directly in the fermenter [24]. Various materials such as heavy metals [22,25], clavulanic acid (a beta-lactam antibiotic) [26,27] have been tested by Amberlite IRA-400. Many of the published studies were examined by the removal of lactic acid using Amberlite IRA-400 by column method [28–32]. Moldes et al. [33] studied the resins (Amberlite IRA-900, IRA-400, IRA-96 and IRA-67) for lactic acid recovery in simultaneous saccharification and fermentation (SSF) processes. Ataei and Vasheghani-Farahani [34] examined in situ separation of lactic acid from fermentation broth using Amberlite resin. Pradhan et al. [24] investigated the adsorption behavior of lactic acid on anionic resins (Amberlite IRA-92, IRA-400 and IRA-425) by batch method. However, little research has been done on the adsorption mechanisms of lactic acid under different operating conditions by batch method.

In the current study, adsorption based on ion-exchange was examined for lactic acid separation from the water using Amberlite IRA-400. Some parameters like adsorption time, the initial lactic acid concentration, Amberlite IRA-400 amount and temperature were investigated. The acquired experimental data were modelled using the adsorption isotherm models including Langmuir, Freundlich and Temkin isotherm models, and kinetic models including the pseudo-first-order, pseudo-second-order kinetic models and Weber-Morris intra-particle diffusion model.

## 2. Materials and methods

The lactic acid (>90%) was supplied by Merck (USA). The lactic acid solutions were prepared by dissolution of the initial acid concentration of about 2% (w/w) (pH = 2.11), 4% (w/w) (pH = 1.90), 6% (w/w) (pH = 1.81), 8% (w/w) (pH = 1.76) and 10% (w/w) (pH = 1.66) in distilled water. Amberlite IRA-400 resin (chloride form) was acquired from Sigma-Aldrich (USA) and was utilized without further treatment. The characteristic of the Amberlite IRA-400 was summarized in Table 1.

In the adsorption experiments, the volume of lactic acid solution of 5 mL was utilized. Aqueous lactic acid solution and a known quantity of Amberlite IRA-400 were added to glass Erlenmeyer. Experiments were conducted by shaking glass Erlenmeyer in thermostatic water bath shaker (Nüve ST 30, Turkey) for the determined optimum time. The shaker speed was 150 rpm. Amberlite IRA-400 was separated from the solution by the filtration method. The concentrations of lactic acid before and after adsorption were analyzed by means of an automatic titrator (SI Analytics, Schott Titroline, Germany) using 0.1 N NaOH solution.

Adsorption capacity ($q_e$, mg $g^{-1}$), the adsorbed quantity of lactic acid by Amberlite IRA-400 at equilibrium, was calculated by means of Eq. (1):

$$q_e = \left[\frac{(C_0 - C_e)}{M}\right] \times V \quad (1)$$

where $C_0$ and $C_e$ (mg $L^{-1}$) represent the concentrations of initial and equilibrium lactic acid, $M$ (g) implies the quantity of adsorbent and $V$ (L) signifies the volume of aqueous lactic acid solution.

## 3. Results and discussion

### 3.1. Determination of optimum adsorption time

At the beginning of adsorption experiments, the optimum adsorption time was determined by using Amberlite IRA-400 of 0.1 g and the initial concentration of lactic acid solution of 10% (w/w) at 25°C. Fig. 1a depicts the effect of time on the lactic acid adsorption by Amberlite IRA-400. It was obvious from Fig. 1a that the adsorption capacity of lactic acid increased with increasing time at the initial stages, then, the adsorption became slow until the equilibrium was reached. At the start, the adsorption is rapid due to the adsorption sites on the adsorbent surface are free. Then, the adsorption becomes slow owing to decreasing in the number of available adsorption sites [35,36]. As illustrated in Fig. 1a, the equilibrium attained about 180 min. Consequently, the optimum adsorption time was determined as 180 min for the next experiments.

### 3.2. Effect of different parameters on the adsorption of lactic acid by Amberlite IRA-400

In the second stage of experimental investigation, the effect of initial lactic acid concentration was examined at the optimum adsorption time. In these experiments, different acid concentrations of about 2% w/w (20.3 g $L^{-1}$), 4% w/w (39.9 g $L^{-1}$), 6% w/w (60.55 g $L^{-1}$), 8% w/w (80.96 g $L^{-1}$) and 10% w/w (100.81 g $L^{-1}$) were used. The adsorbent amount is 0.1 g and the temperature is 25°C. After that, the effect of the amount of adsorbent was detected by using Amberlite IRA-400 of 0.1, 0.2, 0.3, 0.4 and 0.5 g and initial lactic acid concentration of 10% (w/w) 25°C. Finally, the effect of temperature was investigated at the various temperatures of 25°C, 45°C and 65°C. In these experiments, the amount

Table 1
Characteristic of Amberlite IRA-400 resin

| | Properties |
|---|---|
| Matrix | Styrene-divinylbenzene (gel) |
| Functional group | Quaternary ammonium |
| Ionic form | $Cl^-$ |
| Capacity | 1.4 meq $mL^{-1}$ by wetted bed volume |
| Particle size | 600–750 μm |
| Operating pH | 0–14 |

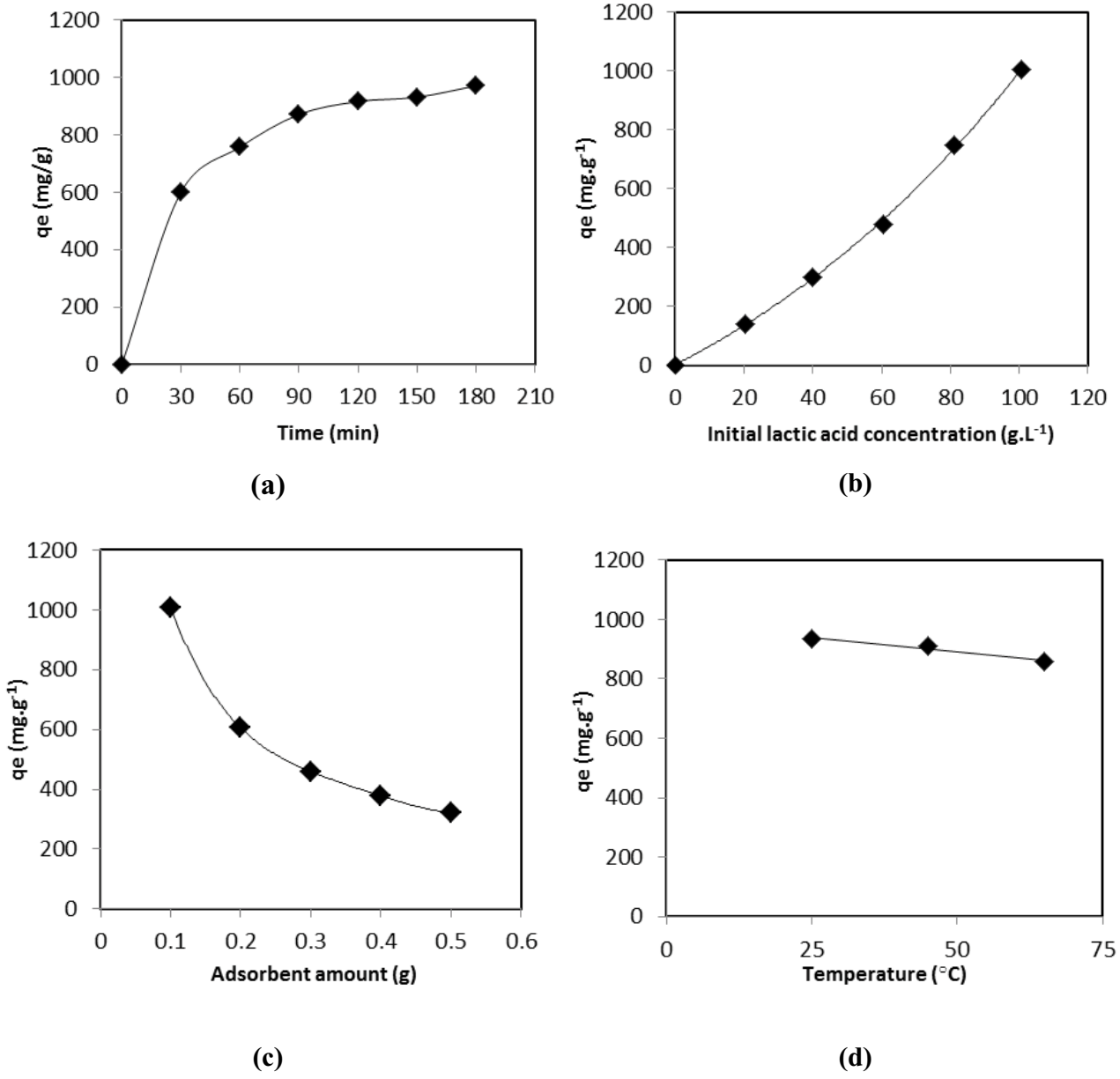


Fig. 1. (a) Effect of contact time, (b) initial acid concentration, (c) adsorbent amount and (d) temperature on the adsorption of lactic acid by Amberlite IRA-400.

of adsorbent is 0.1 g and the concentration of lactic acid is 10% w/w.

Fig. 1 represents the effect of initial lactic acid concentration, adsorbent amount and temperature on the adsorption. From Fig. 1b, the adsorption capacity was increased by increasing the initial concentration of lactic acid. It can be explained by the driving force for mass transfer. As the initial acid concentration increases, the driving force for mass transfer becomes greater, so the adsorption capacity increases [37]. A similar result was obtained by Uslu and Majumder [38] for lactic acid adsorption by Amberlite XAD-7. As can be seen in Fig. 1c, the increase in the amount of Amberlite IRA-400 resulted in decreasing the adsorption capacity. The maximum value of adsorption capacity was obtained as 1,010 mg $g^{-1}$ when the smallest amount of Amberlite IRA-400 (0.1 g) was used. Polowczyk et al. [39] was used Amberlite IRA-400 for the removal of molybdenum(VI) and vanadium(V), and they observed that the adsorption capacity decreased with the increase in resin amount. Furthermore, as shown in Fig. 1d, the adsorption capacity decreased slightly with the increasing temperature. It shows that the lactic acid adsorption is exothermic. Similarly, Fu et al. [40] have investigated the adsorption of fumaric acid by Amberlite IRA-400 and they found that the values of equilibrium adsorption capacity decreased with the increasing temperature.

Amberlite IRA-400 is a strong base resin containing a positive charged quaternary ammonium functional group.

The quaternary ammonium functional group can adsorb both the lactate ion and molecular lactic acid. In this case, the adsorption mechanism of lactic acid varies depending on the degree of ionization of lactic acid in the solution. This is related to the relationship between the pKa value and the pH of the solution. The degree of ionization of lactic acid in the solution can be calculated by the following equation [24,41]:

$$\text{Ionized}\% = \frac{100}{1+\exp^{(\text{pKa}-\text{pH})}} \quad (2)$$

From Eq. (2), the degree of ionization of lactic acid can be obtained as 13.5%, 29.7%, 46.5%, 24.2%, 10.5%, 4.2% and 1.6% for pH 2.0, 3.0, 4.0, 5.0, 6.0, 7.0 and 8.0.

At the pH value (2.0, 6.0, 7.0 or 8.0), the undissociated form of lactic acid is predominant and Amberlite IRA-400 predominantly binds to the molecular lactic acid. At the pH range (3.0–5.0), the dissociated form of lactic acid is predominant, in this case, Amberlite IRA-400 can form ionic bonds with the lactate ion as follows:

$$L^- + R^+Cl^- \leftrightarrow R^+L^- + Cl^- \quad (3)$$

In this equation, L signifies the lactate ion and R symbolizes a cationic quaternary ammonium functional group of the resin. Chloride form ($Cl^-$) of quaternary ammonium of Amberlite IRA-400 has a weak base characteristic. This property facilitates the adsorption of acid through acid-base interaction. In this case, lactic acid adsorption with Amberlite IRA-400 takes place by means of an ion-exchange mechanism [24,42,43]. In this study, under the pH range studied (1.66–2.11), the degree of ionization of lactic acid (9.9%–14.8%), the molecular lactic acid (predominant) and the lactate ion binds to Amberlite IRA-400. Cao et. al [43] studied the adsorption of lactic acid on IRA-400, at the pH above (5.0) and below (2.0) the pKa (3.86) of lactic acid with column separation process. They reported that Amberlite IRA-400 was successfully applied for the separation of lactic acid at pH above and below the pKa (3.86). Raya-Tonetti et al. [32] was also used Amberlite IRA-400 in an upstream fluidized bed column to recover lactic acid directly from fermentation at pH 8.0.

Table 2 shows a comparison of the values of adsorption capacity of Amberlite IRA-400 and various resins for the lactic acid adsorption.

### 3.3. Adsorption isotherm models for lactic acid adsorption by Amberlite IRA-400

The adsorption mechanism is generally described by an isotherm model that correlates the equilibrium concentration of the solid phase (adsorbent) with the equilibrium concentration of the liquid phase (adsorbate). In the current work, the most used isotherm models, Langmuir, Freundlich and Temkin isotherm models were utilized to express and model the adsorption characteristic of lactic acid by Amberlite IRA-400. These isotherms models and equations summarized in Table 3 [17,45].

Fig. 2 illustrates the linear plots of Langmuir, Freundlich and Temkin isotherm models for the adsorption of lactic acid by Amberlite IRA-400. Table 4 shows the parameters of Langmuir, Freundlich and Temkin isotherm models for calculated from the linear plots of isotherm models. Langmuir isotherm model approach assumes that the adsorption occur monolayer on the surface, indicating that the adsorbent surface is homogeneous and has energetically equivalent adsorption sites [46]. As can be seen in Table 4, Langmuir isotherm parameters have negative values, which suggesting that the adsorption mechanism of the studied system does not explain sufficiently by the Langmuir approach [47,48]. Since the Langmuir isotherm model approach is not sufficient to explain the adsorption mechanism, non-linear Langmuir–Freundlich combination isotherm was employed. Langmuir–Freundlich combination isotherm model can be expressed below as [41,49]:

$$\text{Non-linear form}: \quad q_e = \frac{Q_m K C_e^{\frac{1}{n}}}{1 + K C_e^{\frac{1}{n}}} \quad (10)$$

where $Q_m$ is Langmuir adsorption constant related to the adsorption capacity (mg $g^{-1}$), $K$ is equivalent to the Langmuir isotherm constant (L $mg^{-1})^{1/n}$, and $n$ is equivalent to Freundlich adsorption constant related to adsorption intensity. As shown in Table 4, the obtained isotherm model parameters were positive values, which means this isotherm

Table 2
Comparison of adsorption capacities of ion exchange resins for lactic acid adsorption

| Ion exchange resins | Type | Initial lactic acid concentration | Adsorbent dose (g) | Temperature (°C) | Adsorption capacity (mg $g^{-1}$) | References |
|---|---|---|---|---|---|---|
| Amberlite IRA-400 | S | 10% w/w (100.81 g $L^{-1}$) | 0.1 | 25 | 1,010 | This study |
| Amberlite IRA-400 | S | 18 g $L^{-1}$ | 0.5 | 30 | 48 | [24] |
| Amberlite IRA-96 | W | 100 g $L^{-1}$ | 25 | 25 | 210.46 | [42] |
| Amberlite IRA-402 | S | 160 mg lactic acid/5 ml | 1 | 25 | 119 | [44] |
| Amberlite IRA-67 | W | 160 mg lactic acid/5 ml | 1 | 25 | 126 | [44] |
| Amberlite IRA-67 | W | 6.66 g $L^{-1}$ | 5 | 25 | 60.10 | [15] |
| Amberlite IRA-67 | W | 208.98 g $L^{-1}$ | 1 | 25 | 743.20 | [2] |

S: Strong anion exchange resin.
W: Weak anion exchange resin.

Table 3
Adsorption isotherm models

| Isotherm models | Equations | |
|---|---|---|
| Langmuir isotherm model | Non-linear form: $q_e = \frac{Q_m K_L C_e}{1 + K_L C_e}$ | (4) |
| | Linear form: $\frac{C_e}{q_e} = \frac{C_e}{Q_m} + \left(\frac{1}{K_L Q_m}\right)$ | (5) |
| | Plot: $\frac{C_e}{q_e}$ vs. $C_e$ | |
| | $K_L$: Langmuir isotherm constant (L mg$^{-1}$)<br>$Q_m$: Maximum adsorption capacity (mg g$^{-1}$) | |
| Freundlich isotherm model | Non-linear form: $q_e = K_f C_e^{\frac{1}{n}}$ | (6) |
| | Linear form: $\log q_e = \log K_f + \frac{1}{n}\log C_e$ | (7) |
| | Plot: $\log q_e$ *vs.* $\log C_e$ | |
| | $K_f$: Freundlich isotherm constant related to adsorption capacity (mg g$^{-1}$)(L mg$^{-1}$)$^n$<br>$n$: Freundlich isotherm constant related to adsorption intensity | |
| Temkin isotherm model | Non linear form: $q_e = B \ln(K_t C_e)$; $B = \frac{RT}{b_t}$ | (8) |
| | Linear form: $q_e = B \text{ In } K_t + B \ln C_e$ | (9) |
| | Plot: $q_e$ vs. $\ln C_e$ | |
| | $K_t$: Temkin isotherm constant (L g$^{-1}$)<br>$b_t$: Temkin isotherm constant related to adsorption heat (J mol$^{-1}$) | |

model can be used to explain the adsorption. However, as can be seen in Table 4, Freundlich isotherm model was better fitted to the experimental adsorption results due to its having the highest regression coefficient ($R^2 = 0.9935$). Freundlich isotherm model describes the multilayer adsorption on the heterogeneous adsorbent surface. Furthermore, Fig. 3 depicts the comparison of the values of experimental adsorption capacity with the values of adsorption capacity obtained from the parameters of isotherm models. The adsorption capacity of the isotherm models was calculated from non-linear isotherm equations by placing the calculated isotherm parameters given in Table 4. As depicted in Fig. 3, the experimental data were well characterized by Freundlich isotherm model.

### *3.4. Adsorption kinetics models for lactic acid adsorption by Amberlite IRA-400*

Several kinetic models including pseudo-first-order, pseudo-second-order kinetic models and Weber-Morris intra-particle diffusion model were performed to appraise the experimental results of lactic acid adsorption. These kinetics models and their equations were summarized in Table 5 [1,50]. To examine the adsorption kinetics of lactic acid by Amberlite IRA-400, was studied for a period of 180 min for an initial lactic acid concentration of 10% (w/w) at 25°C. The amount of Amberlite IRA-400 was 0.1 g. The values of adsorption capacity were calculated by means of Eq. (1) and also shown in Fig. 1a. After that, the kinetics model parameters were calculated by using experimental adsorption capacity results by means of the equations summarized in Table 5. Fig. 4 demonstrates the linear plots of pseudo-first-order, pseudo-second-order and Weber-Morris intra-particle models for the adsorption of lactic acid by Amberlite IRA-400. The kinetic parameters calculated from the linear plots of models for the adsorption of lactic acid on Amberlite IRA-400 are shown in Table 6. The results given in Table 6 indicated that among these three models, pseudo-second-order kinetic model had the highest $R^2$ value. So, pseudo-second-order kinetic model was well fitted the experimental data owing to the highest $R^2$ value of 0.9992. Pseudo-second-order kinetic model indicates that the adsorption mechanism depends on the adsorbent and adsorbate [46,51].

## 4. Conclusion

Amberlite IRA-400 resin has been successfully performed for the recovery of lactic acid from the water. The current adsorption study showed that the strong base resin Amberlite IRA-400 had a high affinity for lactic acid uptake. The adsorption experiments indicated that the adsorption capacity increased with the increasing the initial lactic acid

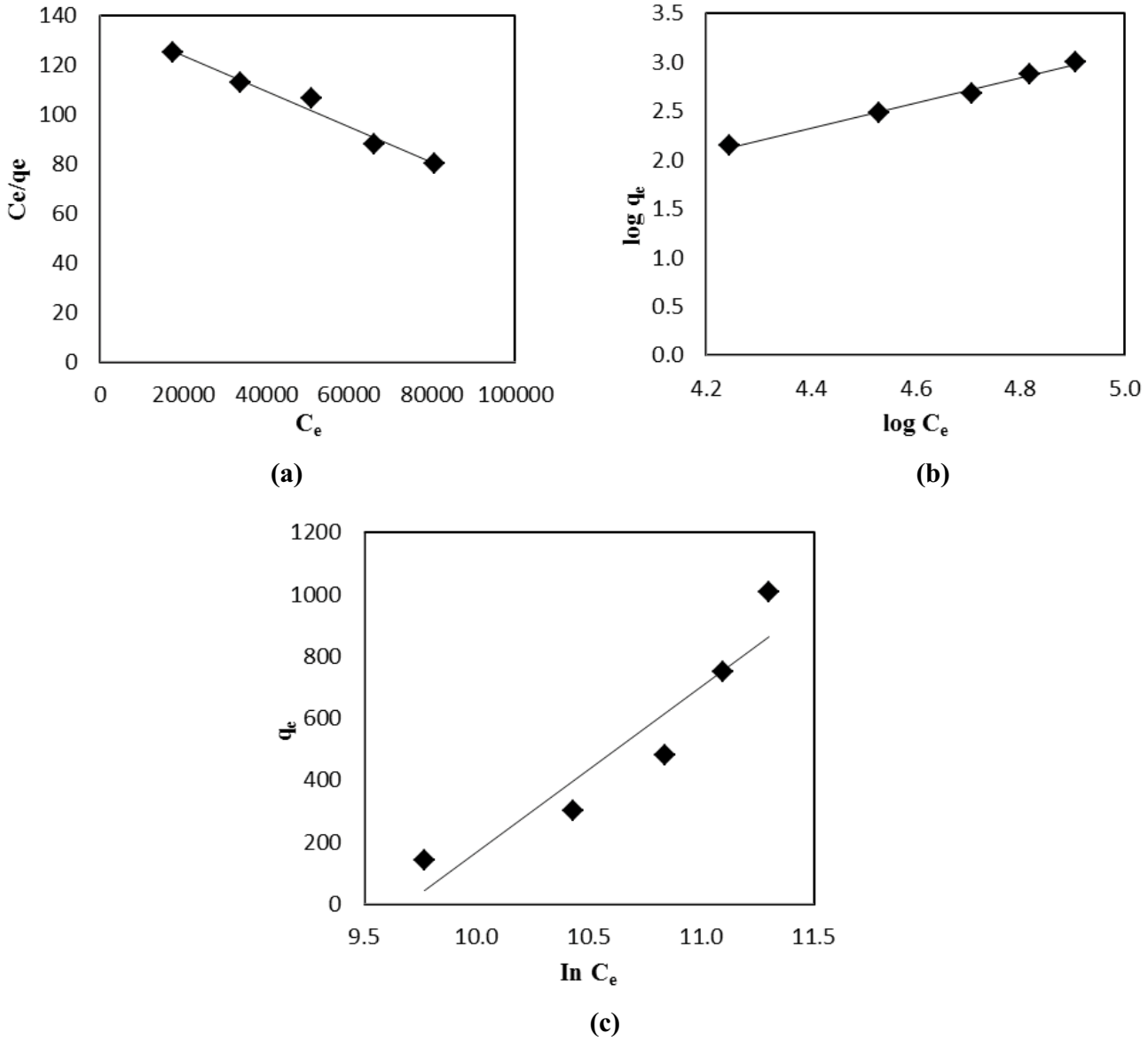


Fig. 2. Linear fits of (a) Langmuir, (b) Freundlich and (c) Temkin isotherm models for the adsorption of lactic acid by Amberlite IRA-400.

Table 4
Parameters of Langmuir, Freundlich, Langmuir–Freundlich and Temkin isotherm models for lactic acid adsorption by Amberlite IRA-400

| Isotherm models | Isotherm parameters and regression coefficients | | | |
|---|---|---|---|---|
| Langmuir isotherm model | $Q_m$ (mg g$^{-1}$) | $K_L$ (L mg$^{-1}$) | | $R^2$ |
| | –1,428.5 | $-5.06 \times 10^{-6}$ | | 0.9763 |
| Freundlich isotherm model | $K_f$ (mg g$^{-1}$)(L mg$^{-1}$)$^n$ | $n$ | | $R^2$ |
| | $4.9 \times 10^{-4}$ | 0.78 | | 0.9935 |
| Langmuir-Freundlich combination isotherm model | $Q_m$ (mg g$^{-1}$) | $K$ (L mg$^{-1}$)$^{1/n}$ | $n$ | $R^2$ |
| | 1,005.5 | $1.202 \times 10^{-13}$ | 0.36 | 0.9898 |
| Temkin isotherm model | $K_t$ (L g$^{-1}$) | $b_t$ (J mol$^{-1}$) | | $R^2$ |
| | $6.19 \times 10^{-5}$ | 4.62 | | 0.8799 |

Table 5
Adsorption kinetic models

| Kinetic models | Equations | |
|---|---|---|
| Pseudo-first-order model | Non-linear form: $\frac{dq_t}{dt} = k_1(q_e - q_t)$ | (11) |
| | Linear form: $\ln(q_e - q_t) = \ln q_e - k_1 t$ | (12) |
| | Plot: $\ln(q_e - q_t)$ vs. $t$ | |
| | $k_1$: Kinetic rate coefficient of pseudo-first-order ($min^{-1}$) | |
| Pseudo-second-order model | Non-linear form: $\frac{dq_t}{dt} = k_2(q_e - q_t)^2$ | (13) |
| | Linear form: $\frac{t}{q_t} = \frac{1}{k_2 q_e^2} + \frac{t}{q_e}$ | (14) |
| | Plot: $\frac{t}{q_t}$ vs. $t$ | |
| | $k_2$: Kinetic rate coefficient of pseudo-second-order (g $mg^{-1}$ $min^{-1}$) | |
| Weber-Morris intra-particle diffusion model | $q_t = k_{id} t^{\frac{1}{2}} + C$ | (15) |
| | *Plot*: $q_t$ vs. $t^{\frac{1}{2}}$ | |
| | $k_{id}$: Intra-particle diffusion rate coefficient (mg $g^{-1}$ $min^{-1/2}$) | |
| | $C$: Intercept related to the thickness of boundary layer | |
| Notes | $q_e$: Adsorption capacity of the adsorbent at the equilibrium (mg $g^{-1}$) | |
| | $q_t$: Adsorption capacity of the adsorbent at the time ($t$) (mg $g^{-1}$) | |

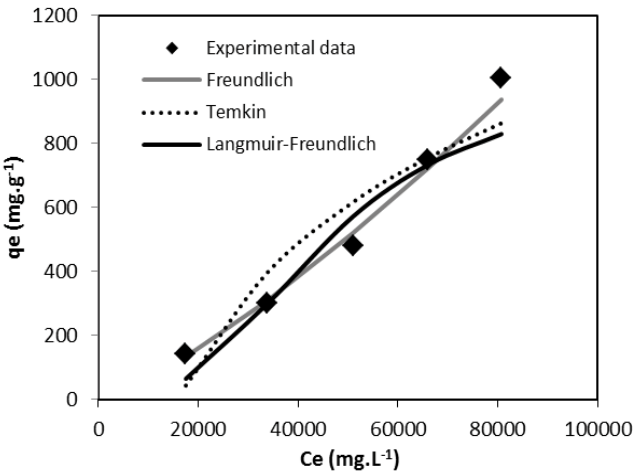


Fig. 3. Comparison of the values of experimental adsorption capacity with values of the adsorption capacity calculated from isotherm models.

concentration, and also the adsorption capacity decreased with the increasing Amberlite IRA-400 amount. In addition to, the increase in temperature resulted in decreasing adsorption capacity, indicating the lactic acid adsorption with Amberlite IRA-400 is exothermic. The maximum adsorption capacity for lactic acid removal was obtained to be 1,010 mg $g^{-1}$ at the experimental conditions conducted as the initial acid concentration of 10% w/w (1.12 mol $L^{-1}$), the amount of Amberlite IRA-400 of 0.1 g and the temperature of 25°C. Freundlich adsorption isotherm model fitted experimental results quite well. Lactic acid recovery was well characterized by the pseudo-second-order kinetic model.

Table 6
Kinetic model parameters for lactic acid adsorption by Amberlite IRA-400

| Kinetic models | Kinetic parameters and regression coefficients | | |
|---|---|---|---|
| Pseudo-first-order model | $k_1$ ($min^{-1}$) 0.0194 | $q_e$ (mg $g^{-1}$) 641 | $R^2$ 0.9848 |
| Pseudo-second-order model | $k_2$ (g $mg^{-1}$ $min^{-1}$) $3.4 \times 10^{-5}$ | $q_e$ (mg $g^{-1}$) 1,111 | $R^2$ 0.9992 |
| Weber-Morris intra-particle diffusion model | $k_{id}$ (mg $g^{-1}$ $min^{-1/2}$) 45.76 | | $R^2$ 0.9375 |

**Acknowledgement**

This study was funded by İstanbul University with the Project Number 20671.

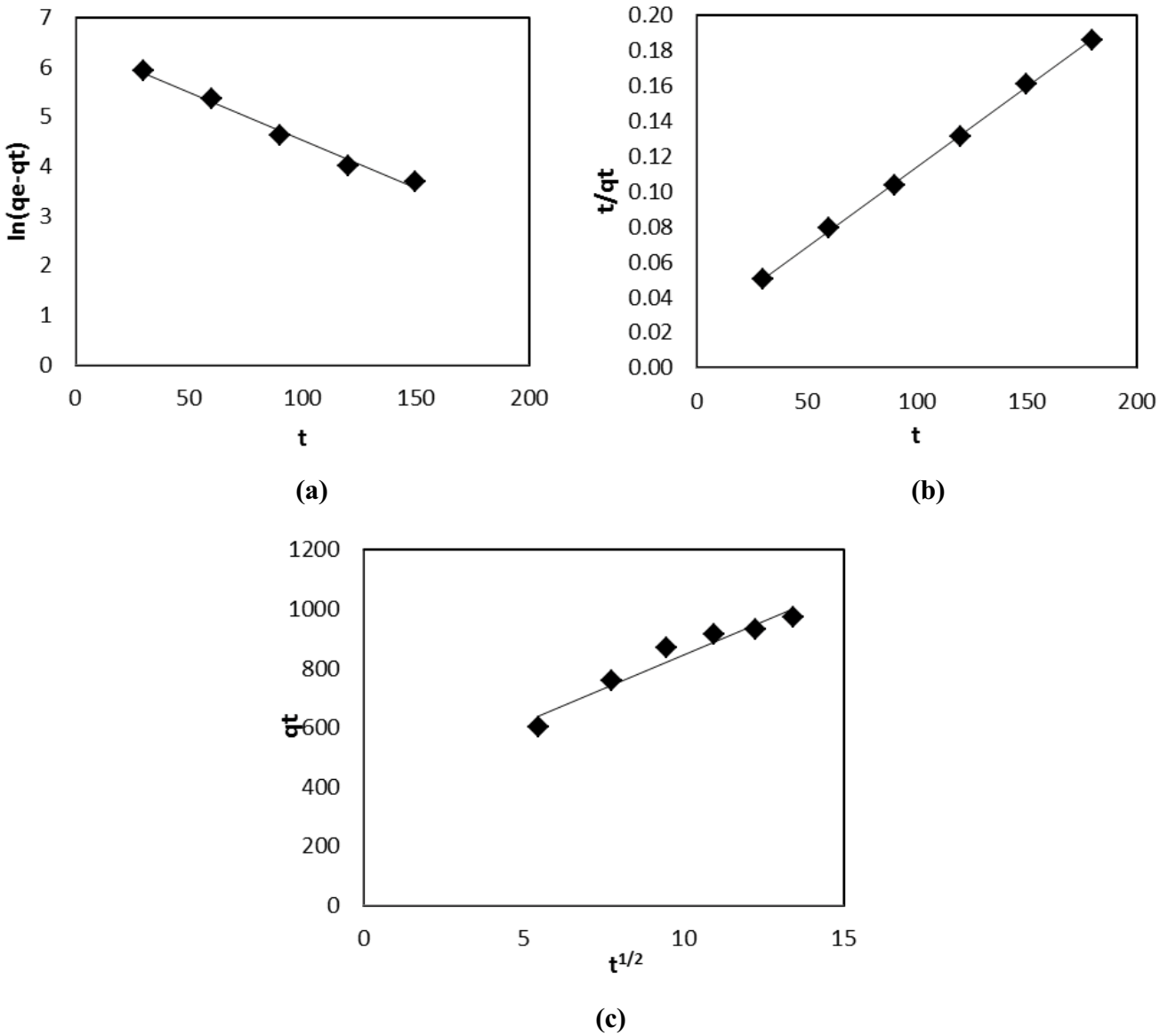


Fig. 4. Linear fits of (a) pseudo-first-order kinetic model, (b) pseudo-second-order kinetic model and (c) Weber-Morris intra-particle diffusion model for the adsorption of lactic acid by Amberlite IRA-400.

## References


[1] İ. İlalan, İ. İnci, N. Baylan, Separation of lactic acid by multiwall carbon nanotube adsorption from water, Desal. Wat. Treat., 93 (2017) 339–345.

[2] Ş.S. Bayazit, İ. İnci, H. Uslu, Adsorption of lactic acid from model fermentation broth onto activated carbon and Amberlite IRA-67, J. Chem. Eng. Data, 56 (2011) 1751–1754.

[3] K.L. Wasewar, A.A. Yawalkar, J.A. Moulijn, V.G. Pangarkar, Fermentation of glucose to lactic acid coupled with reactive extraction: a review, Ind. Eng. Chem. Res., 43 (2004) 5969–5982.

[4] M. Marinova, G. Kyuchoukov, J. Albet, J. Molinier, G. Malmary, Separation of tartaric and lactic acids by means of solvent extraction, Sep. Purif. Technol., 37 (2004) 199–207.

[5] J. Marták, Š. Schlosser, Extraction of lactic acid by phosphonium ionic liquids, Sep. Purif. Technol., 57 (2007) 483–494.

[6] K.L. Wasewar, A.B.M. Heesink, G.F. Versteeg, V.G. Pangarkar, Reactive extraction of lactic acid using alamine 336 in MIBK: equilibria and kinetics, J. Biotechnol., 97 (2002) 59–68.

[7] Ş.S. Bayazit, H. Uslu, İ. İnci, Comparison of the efficiencies of amine extractants on lactic acid with different organic solvents, J. Chem. Eng. Data, 56 (2009) 750–756.

[8] M.C.M. Cockrem, P.D. Johnson, Recovery of Lactate Esters and Lactic Acid from Fermentation Broth, Google Patents, 1993.

[9] R. Kumar, H. Nanavati, S.B. Noronha, S.M. Mahajani, A continuous process for the recovery of lactic acid by reactive distillation, J. Chem. Technol. Biotechnol., 81 (2006) 1767–1777.

[10] Y. Li, A. Shahbazi, K. Williams, C. Wan, Separate and concentrate lactic acid using combination of nanofiltration and reverse osmosis membranes, Appl. Biochem. Biotechnol., 147 (2008) 1–9.

[11] R.A. Diltz, T.V. Marolla, M.V. Henley, L.X. Li, Reverse osmosis processing of organic model compounds and fermentation broths, Bioresour. Technol., 98 (2007) 686–695.

[12] Y.H. Kim, S.-H. Moon, Lactic acid recovery from fermentation broth using one-stage electrodialysis, J. Chem. Technol. Biotechnol., 76 (2001) 169–178.

[13] P. Boyaval, C. Corre, S. Terre, Continuous lactic acid fermentation with concentrated product recovery by ultrafiltration and electrodialysis, Biotechnol. Lett., 9 (1987) 207–212.
[14] Y. Li, A. Shahbazi, Lactic Acid Recovery From Cheese Whey Fermentation Broth Using Combined Ultrafiltration and Nanofiltration Membranes, Twenty-Seventh Symposium on Biotechnology for Fuels and Chemicals, Springer, USA, 2006, 985–996.
[15] A. Yousuf, F. Bonk, J.-R. Bastidas-Oyanedel, J.E. Schmidt, Recovery of carboxylic acids produced during dark fermentation of food waste by adsorption on Amberlite IRA-67 and activated carbon, Bioresour. Technol., 217 (2016) 137–140.
[16] M. Lalikoğlu, A. Gök, M.K. Gök, Y.S. Aşçı, Investigation of lactic acid separation by layered double hydroxide: equilibrium, kinetics, and thermodynamics, J. Chem. Eng. Data, 60 (2015) 3159–3165.
[17] N. Baylan, A.E. Meriçboyu, Adsorption of lead and copper on bentonite and grapeseed activated carbon in single- and binary-ion systems, Sep. Sci. Technol., 51 (2016) 2360–2368.
[18] Md. Rabiul Awual, G.E. Eldesoky, T. Yaita, Mu. Naushad, H. Shiwaku, Z.A. AlOthman, S. Suzuki, Schiff based ligand containing nano-composite adsorbent for optical copper(II) ions removal from aqueous solutions, Chem. Eng. J., 279 (2015) 639–647.
[19] A.B. Albadarin, M.N. Collins, Mu. Naushad, S. Shirazian, G. Walker, C. Mangwandi, Activated lignin-chitosan extruded blends for efficient adsorption of methylene blue, Chem. Eng. J., 307 (2017) 264–272.
[20] I.H. Aljundi, J.M. Belovich, O. Talu, Adsorption of lactic acid from fermentation broth and aqueous solutions on Zeolite molecular sieves, Chem. Eng. Sci., 60 (2005) 5004–5009.
[21] C. Chen, L.-K. Ju, Coupled lactic acid fermentation and adsorption, Appl. Microbiol. Biotechnol., 59 (2002) 170–174.
[22] S. Mustafa, T. Ahmad, A. Naeem, K.H. Shah, M. Waseem, Kinetics of chromium ion removal from tannery wastes using amberlite IRA-400 $Cl^-$ and its hybrids, Water Air Soil Pollut., 210 (2010) 43–50.
[23] A.M. Khan, S. Gautam, S.A. Ganai, Sorption studies on cresol red modified Amberlite IR400 ($Cl^-$) resin: Binary and selective separation of $Hg^{2+}$ ions, Indian J. Chem. Technol., 15 (2008) 541–546.
[24] N. Pradhan, E.R. Rene, P.N.L. Lens, L. Dipasquale, G. d'Ippolito, A. Fontana, A. Panico, G. Esposito, Adsorption behaviour of lactic acid on granular activated carbon and anionic resins: thermodynamics, isotherms and kinetic studies, Energies, 10 (2017) 665.
[25] Mu. Naushad, S. Vasudevan, G. Sharma, A. Kumar, Z. ALOthman, Adsorption kinetics, isotherms, and thermodynamic studies for $Hg^{2+}$ adsorption from aqueous medium using alizarin red-S-loaded Amberlite IRA-400 resin, Desal. Wat. Treat., 57 (2016) 18551–18559.
[26] M. Barboza, R.M.R.G. Almeida, C.O. Hokka, Influence of temperature on the kinetics of adsorption and desorption of clavulanic acid by ionic exchange, Biochem. Eng. J., 14 (2003) 19–26.
[27] M. Barboza, R.M.R.G. Almeida, C.O. Hokka, Intrinsic kinetic parameters of clavulanic acid adsorption by ion-exchange chromatography, Ind. Eng. Chem. Res., 41 (2002) 5789–5793.
[28] A.V. Sosa, P.R. Córdoba, N.I. Perotti, Fluidized bed design parameters affecting novel lactic acid downstream processing, Biotechnol. Progr., 17 (2001) 1079–1083.
[29] A.B. Moldes, J.L. Alonso, J.C. Parajó, Resin selection and single-step production and recovery of lactic acid from pretreated wood, Biotechnol. Appl. Biochem., 95 (2001) 69–81.
[30] P. Gluszcz, T. Jamroz, B. Sencio, S. Ledakowicz, Equilibrium and dynamic investigations of organic acids adsorption onto ion-exchange resins, Bioprocess Biosyst. Eng., 26 (2004) 185–190.
[31] A.V. Sosa, J. Ochoa, N.I. Perotti, Modeling of direct recovery of lactic acid from whole broths by ion exchange adsorption, Bioseparation, 9 (2000) 283–289.
[32] G. Raya-Tonetti, P. Córdoba, J. Bruno-bárcena, F. Siñeriz, N. Perotti, Fluidized bed ion exchange for improving purification of lactic acid from fermentation, Biotechnol. Tech., 13 (1999) 201–205.
[33] A.B. Moldes, J.L. Alonso, J.C. Parajó, Recovery of lactic acid from simultaneous saccharification and fermentation media using anion exchange resins, Bioprocess Biosyst. Eng., 25 (2003) 357–363.
[34] S.A. Ataei, E. Vasheghani-Farahani, In situ separation of lactic acid from fermentation broth using ion exchange resins, J. Ind. Microbiol. Biotechnol., 35 (2008) 1229.
[35] A.A. Alqadami, Mu. Naushad, Z.A. Alothman, A.A. Ghfar, Novel metal–organic framework (MOF) based composite material for the sequestration of U(VI) and Th(IV) metal ions from aqueous environment, ACS Appl. Mater. Interfaces, 9 (2017) 36026–36037.
[36] M. Naushad, Surfactant assisted nano-composite cation exchanger: development, characterization and applications for the removal of toxic $Pb^{2+}$ from aqueous medium, Chem. Eng. J., 235 (2014) 100–108.
[37] Mu. Naushad, T. Ahamad, B.M. Al-Maswari, A.A. Alqadami, S.M. Alshehri, Nickel ferrite bearing nitrogen-doped mesoporous carbon as efficient adsorbent for the removal of highly toxic metal ion from aqueous medium, Chem. Eng. J., 330 (2017) 1351–1360.
[38] H. Uslu, S. Majumder, Adsorption studies of lactic acid by polymeric adsorbent Amberlite XAD-7: equilibrium and kinetics, J. Chem. Eng. Data, 62 (2017) 1501–1506.
[39] I. Polowczyk, P. Cyganowski, B.F. Urbano, B.L. Rivas, M. Bryjak, N. Kabay, Amberlite IRA-400 and IRA-743 chelating resins for the sorption and recovery of molybdenum(VI) and vanadium(V): equilibrium and kinetic studies, Hydrometallurgy, 169 (2017) 496–507.
[40] Y.-Q. Fu, H.Y. Zhu, R. Jiang, L.-F. Yin, A.-G. Ying, S.-B. Ren, Q.-C. Ruan, Adsorptive separation of fumaric acid and glucose from the mixed aqueous solutions by anion exchange resin Amberlite IRA-400, J. Indian Chem. Soc., 60 (2013) 73–77.
[41] M.J. Dethe, K.V. Marathe, V.G. Gaikar, Adsorption of lactic acid on weak base polymeric resins, Sep. Sci. Technol., 41 (2006) 2947–2971.
[42] M. Bishai, S. De, B. Adhikari, R. Banerjee, A platform technology of recovery of lactic acid from a fermentation broth of novel substrate *Zizyphus oenophlia*, 3 Biotech, 5 (2015) 455–463.
[43] X.J. Cao, H.S. Yun, Y.-M. Koo, Recovery of L-(+)-lactic acid by anion exchange resin Amberlite IRA-400, Biochem. Eng. J., 11 (2002) 189–196.
[44] R.P. John, K.M. Nampoothiri, A. Pandey, L(+)-Lactic acid recovery from cassava bagasse based fermented medium using anion exchange resins, Braz. Arch. Biol. Technol., 51 (2008) 1241–1248.
[45] Ş.S. Bayazit, İ. İnci, Adsorption of Pb(II) ions from aqueous solutions by carbon nanotubes oxidized different methods, J. Ind. Eng. Chem., 19 (2013) 2064–2071.
[46] B. Meroufel, O. Benali, M. Benyahia, Y. Benmoussa, M. Zenasni, Adsorptive removal of anionic dye from aqueous solutions by Algerian kaolin: characteristics, isotherm, kinetic and thermodynamic studies, J. Mater. Environ. Sci., 4 (2013) 482–491.
[47] J. Kiurski, S. Adamović, I. Oros, J. Krstić, I. Kovačević, Adsorption feasibility in the Cr(total) ions removal from waste printing developer, Global Nest J., 14 (2012) 18–23.
[48] S. Jemutai-Kimosop, V.A. Okello, F. Orata, Z.M. Getenga, V.O. Shikuku, Green remediation of carbamazepine from water using novel magnetic iron modified carbonized baggasse: kinetics, equilibrium and mechanistic studies, Chem. Sci. Int. J., 18 (2017) 1–9.
[49] K.-W. Jung, K.-H. Ahn, Fabrication of porosity-enhanced MgO/biochar for removal of phosphate from aqueous solution: application of a novel combined electrochemical modification method, Bioresour. Technol., 200 (2016) 1029–1032.
[50] Z.A. Al-Othman, R. Ali, Mu. Naushad, Hexavalent chromium removal from aqueous medium by activated carbon prepared from peanut shell: adsorption kinetics, equilibrium and thermodynamic studies, Chem. Eng. J., 184 (2012) 238–247.
[51] F.A. Pavan, S.L.P. Dias, E.C. Lima, E.V. Benvenutti, Removal of Congo red from aqueous solution by anilinepropylsilica xerogel, Dyes Pigm., 76 (2008) 64–69.